Research Article

Wenhui Cui*, Wei Qu, Min Jiang, and Gang Yao

The atmospheric model of neural networks based on the improved Levenberg-Marquardt algorithm

Abstract: Traditional atmospheric models are based on the analysis and fitting of various factors influencing the space atmosphere density. Neural network models do not specifically analyze the polynomials of each influencing factor in the atmospheric model, but use large data sets for network construction. Two traditional atmospheric model algorithms are analyzed, the main factors affecting the atmospheric model are identified, and an atmospheric model based on neural networks containing various influencing factors is proposed. According to the simulation error, the Levenberg-Marquardt algorithm is used to iteratively realize the rapid network weight correction, and the optimal neural network atmospheric model is obtained. The space atmosphere is simulated and calculated with an atmospheric model based on neural networks, and its average error rate is lower than that of traditional atmospheric models such as the DTM2013 model and the MSIS00 model. At the same time, the calculation complexity of the atmospheric model based on the neural networks is significantly simplified than that of the traditional atmospheric model.

Keywords: improved Levenberg-Marquardt algorithm; neural networks; atmospheric model

1 Introduction

Recently, with the development of constellation theory and application technology, a variety of low-earth orbit communication constellations began to be deployed (Xu and Zhang 2018). High precision orbit calculation of low-Earth orbit satellites has become a matter of great concern once again. For low orbit satellites, atmospheric resistance is one of the main perturbation factors, and the model accuracy of atmospheric density in low earth orbit directly affects the calculation accuracy of low earth orbit (Hatten et al. 2017). Since the 1960s, various factors affecting atmospheric models have been summarized, and a variety of empirical models of atmospheric density have been established. There are two main kinds of traditional atmospheric models. In the first category, only the change of atmospheric density with the ground height was considered, such as the exponential model, the improved Harris-Priester model (Montenbruck and Gill 2001). In the second

category, not only the influence of height but the influence of longitude, latitude, and different periods was were taken into accounts, such as the Jacchia series model (Jacchia 1970), the DTM series model (Berger et al. 1998), and the MSIS series model (Hedin et al. 1977). Through the long-term accumulation and analysis of historical measurement data, these models have formed linear or nonlinear polynomials for different atmospheric factors. These models have relatively stable accuracy and are suitable for global atmospheric prediction. The common disadvantages of these models are their low accuracy. The error rates are generally more than 10-15% when the influencing factors are stable (Marcos et al. 1994). The errors are usually about 30% when the various influencing factors are of high disturbance, and the errors are even as high as 100% in some years (Sarah et al. 2002).

With the development of neural networks and data mining technology, researchers have tried to combine data mining, artificial intelligence, and atmospheric models, spacecraft orbit calculations, and other technologies to improve the accuracy of spacecraft orbits and atmospheric calculations. Tang et al. (2001) predicted the atmospheric circulation over the Pacific Ocean by using neural networks, and the results were superior to that of linear regression. Zhang et al. (2014) solved the resource scheduling problem of the Beidou constellation by intelligent distribution algorithm. Cao et al. (2015) improved the accuracy of position

Corresponding Author: Wenhui Cui State Key Laboratory of Astronautic Dynamics, Xi'an 710043, China, E-mail: cwenh_80@163.com, Tel: +86-18092308590
Wei Qu Aerospace Engineering University, Beijing 101416, China
Min Jiang State Key Laboratory of Astronautic Dynamics, Xi'an 710043, China
Gang Yao Beijing Institute of Tracking and Telecommunications Technology, Beijing 100094, China

and attitude estimation of satellite formation by an intelligent unscented predictive filter. Rosangela et al. (2015) used neural networks to perform data assimilation of atmospheric circulation model and achieved encouraging results. Jiang et al. (2017); Jiang (2018) studied the stability of small satellites in the gravitational field of small celestial bodies by intelligent classification. Liao et al. (2018) used the spacecraft orbit data as the benchmark to form the inversion error model, modified the space atmosphere model based on the data mining method and improved the accuracy of the atmosphere model.

2 Factors affecting the density of space atmosphere

The NRLmsise-00 model (hereinafter abbreviated to the MSIS00 model) proposed by the United States Naval Research Laboratory (NRL) in 2000 (Picone et al. 2002) and the DTM2013 Model (Bruinsma 2015) released by ATMOP (Advanced Thermosphere Model and Orbit Prediction project) in 2013 are the two widely used high precision atmospheric model. Since the vertical distribution of atmospheric temperature determines the vertical distribution of atmospheric density, various atmospheric models use the upper atmosphere temperature as the representation of atmospheric density (Li 1995). Both the two atmospheric models calculate the atmospheric density by calculating the atmospheric temperature.

For the DTM2013 model, the atmospheric density at the height Z is:

$$\rho(Z) = \sum i\rho_i(120 \ km)f_i(Z)\exp(G_i(L)) \quad (1)$$

Where, $\rho_i(120 \ km)$ are the density of atmosphere ingredients at the height 120 km. The ingredients include O, O_2, H, He, N, N_2. 120 km is the minimum limit of DTM models. $f_i(Z) = (T_{120}/T(Z))^{1+\alpha+y_i}\exp(-\sigma y_i\zeta)$, where T_{120} is the absolute temperature at the height of 120 km, $T(Z)$ is the absolute temperature at the height Z. $G_i(L)$ is the atmospheric ingredient density correction term based on periodic and non-periodic factors. The non-periodic terms include the latitude term, the solar activity term, and the geomagnetic activity term. The periodic terms include the annual term, semiannual term, diurnal term, and semidiurnal term. The parameters of $G_i(L)$ include the coefficients a_i, the associate Legendre polynomial coefficient P_{mm} based on the solar incidence Angle, the solar radiation proxy of the last day, the mean of F_{30} in 81 days $\bar{F}_{30}$, the geomagnetic index K_P in 3 hours, the mean of K_P in day $\bar{K}_P$, the day of year d.

For the MSIS00 atmospheric model, the temperature of atmosphere where the space higher than 117.2 km is:

$$T_{(z)} = T_\omega + (T_\omega - T_L)e^{-\delta\times\epsilon(Z,Z_L)} \quad (2)$$

Where $\epsilon(Z, Z_L)$ is determined by the height Z and latitude B, $\epsilon(Z, Z_L) = \frac{(Z-Z_L)(R_P+Z_L)}{R_P+Z}$, $R_P = \frac{2\times980.616\times10^{-5}\times(1-0.0026373\times\cos(2B))}{3.085462\times10^{-6}+2.27\times10^{-9}\times\cos(2B)}$, $Z_L = 120$ km. The low order spherical harmonic function fitted with the measured atmospheric data in space is:

$$G_i(L) = P^i_{(31)} + \sum_{j=1}^{13} T_j \quad (3)$$

Where $P^i_{(31)}$ is the fitting constant, which is obtained from the parameter table. T_1 is the solar term (the solar radiation proxy use $F_{10.7}$). T_3 is the symmetrical annual term. T_4 is the symmetrical semi-annual term. T_5 is the asymmetrical annual term. T_6 is the asymmetrical semi-annual term. T_7 is the diurnal term. T_8 is the semidiurnal term. T_9 is the geomagnetic term (the geomagnetic index use A_P). T_{10} is the terdiurnal term. T_{11} is the longitude term. T_{12} is the hybrid term of time and longitude. T_{13} is the hybrid term of time, longitude, and geomagnetic (Picone et al. 2002).

For the space that lower than 117.2 km, the temperature is calculated by interpolation at five height nodes ($Z_1 = 120 \ km, Z_2 = 110 \ km, Z_3 = 100 \ km, Z_4 = 90 \ km, Z_5 = 72.5 \ km$). The function of latitude such as $\epsilon(Z, Z_1)$ and $\epsilon(Z_5, Z_1)$ are used in the temperature function $T_{(Z)}$. The $GS(P^i)$ function is used in the fitting item of the node function $T_{(Z)}$, and it can be written as:

$$GS(P^i) = \sum_{J=1}^{11} T_J \quad (4)$$

Where T_1 is the solar term (the solar radiation proxy use $F_{10.7}$). T_3 is the symmetrical annual term. T_4 is the symmetrical semi-annual term. T_5 is the asymmetrical annual term. T_6 is the asymmetrical semi-annual term. T_7 is the diurnal term. T_8 is the semidiurnal term. T_9 is the geomagnetic term (the geomagnetic index use A_P). T_{10} is the terdiurnal term. T_{11} is the longitude term.

Based on the analysis, the influence term distribution of a spherical harmonic function of the DTM2013 model and the MSIS00 model is completely consistent. In these two models, the measurement time (including annual item, semi-annual item, diurnal item, semidiurnal item, terdiurnal item), longitude, latitude, height, solar radiation proxies, and geomagnetic indices are included. Therefore, the algorithm of the DTM2013 model and the MSIS00 model is to calculate the atmospheric temperature at a certain height in the space indirectly and then obtain the atmospheric

density. The atmospheric temperature at a certain location is a function of the parameters such as height, measurement time, longitude, latitude, solar radiation proxy (and its 81-day mean), geomagnetic index (and its daily mean), etc. The function of atmospheric density and influencing factors is:

$$\rho_{Atmos} = f(t, longi, lati, Z, SRP, GI) \qquad (5)$$

Since the DTM2013 model and the MSIS00 model are all semiempirical models, the polynomials and coefficients of $f(t, longi, lati, Z, SRP, GI)$ are derived by analyzing and fitting historical measured data.

The process of constructing the atmospheric model with the influencing factors can be transformed into a training process of neural networks if the $f(t, longi, lati, Z, SRP, GI)$ is seen as the model of a neural networks. A part of the historical measured atmospheric data is selected randomly to form the training data set. The parameters such as time, longitude, latitude, height, solar radiation proxies, geomagnetic indices in the training set are taken as the input parameters, and the measured atmospheric density data is taken as the expected output to train the neural networks. So the trained neural networks is the atmospheric model based on neural networks. Taking the left measured data as the test data set, the input parameters are substituted into the atmospheric model based on the neural networks to calculate the simulation results of atmospheric density. The model error rate of the neural networks can be obtained by comparing the measured density and the simulation results. Taking the minimum MAE rate as the target, the optimal neural networks atmosphere model can be obtained through iterative training and the parameters correction by error back propagation.

The solar radiation proxy F_{30} and geomagnetic index K_P are used in the DTM2013 model, and the solar radiation proxy $F_{10.7}$ and geomagnetic index A_P are used in the MSIS00 model. There are four combinations of different solar radiation proxies and geomagnetic indices in the atmospheric model based on neural networks. To simplify the problem, K_P index is matched with F_{30} and $F_{10.7}$ proxy to complete atmospheric modeling. Due to the equivalence of A_P index and K_P index (Leif 1976), the accuracy and adaptability of the model use K_P index apply to the model that use A_P index.

3 Atmospheric density data sets based on the GOCE measured data and neural networks

GOCE (Gravity field and steady-state Ocean Circulation Explorer) is a low-orbit satellite launched by the European Space Agency (ESA) in 2009, which is mainly used to detect the earth gravity field and Ocean Circulation. It is equipped with a highly sensitive gravimetric gradiometer capable of making three-dimensional measurements of changes of earth gravity field. The orbital period of GOCE is about 1.6 hours. ESA has released GOCE measured data as public products for precision atmospheric models (Bruinsma et al. 2015).

The measured data of GOCE include measured time, longitude, latitude, height, measured atmospheric density, and so on. These data can be combined with the measured data of solar radiation flux released by the NOAA (National Oceanic and Atmospheric Administration) (Wang et al. 2014) and the measured geomagnetic indices data released by the NGDC (National Geophysical Data Center) to construct two complete data sets of space atmosphere.

The atmospheric data measured by GOCE for 3 years from November 2009 to November 2012 was fused with two solar radiation proxies ($F_{10.7}$ and F_{30}) and geomagnetic index K_P. The data are divided into two data sets according to different solar radiation proxies. Data set 1 includes: measured time, longitude, latitude, height, $F_{10.7}$ proxy, 81-day mean of $F_{10.7}$, 3-hour geomagnetic index K_P, daily mean of K_P and measured atmospheric density. The data set 2 includes: measured time, longitude, latitude, height, F_{30} proxy, 81-day mean of F_{30}, 3-hour geomagnetic index K_P, daily mean of K_P and measured atmospheric density.

Error Back Propagation was proposed by James et al. (1987) of the PDP (Parallel Distributed Procession) group firstly. Neural networks adopted the algorithm of Error Back Propagation to adjust the weights of the networks, which solved the learning problem of multi-layer neural networks and greatly promoted the development of neural networks. In the neural networks, the input layer, the hidden layers, and the output layer are connected, and the neurons in the same layer are isolated. The improved LM (Levenberg-Marquardt) algorithm (Lera and Pinzolas 2002) is adopted for the specific networks learning method. The main idea of the LM algorithm is: Suppose the number of neurons in the input layer are M, the number of neurons in the hidden layers are I, the number of neurons in the output layer are J, the $m - th$ neuron of input layer is x_m, the $i_t h$ neuron of hidden layer is k_i, the $j - th$ neuron of output

layer is y_j. The connection weight from x_m to k_i is ω_{mi}, and weight matrix from k_i to y_j in the hidden layers is ω_{ij}. The weight matrix IW of input layer is composed by ω_{mi}, and the weight matrix LW of hidden layer is composed by ω_{ij}. For the $n + 1$ iteration process, there are:

$$IW(n + 1) = IW(n) - H^{-1}(n)g(n) \qquad (6)$$

$$LW(n + 1) = LW(n) - H^{-1}(n)g(n) \qquad (7)$$

where H is the Hessian matrix of the error performance function, g is the gradient. For the binary differentiable function $f(x, y)$, the Hessian matrix is:

$$H = \begin{bmatrix} \frac{\partial^2 f}{\partial x^2} & \frac{\partial^2 f}{\partial x \partial y} \\ \frac{\partial^2 f}{\partial y \partial x} & \frac{\partial^2 f}{\partial y^2} \end{bmatrix}$$

The Hessian matrix of the multiple variables function is analogous. When the error performance function has the form of squared error, the Hessian matrix can be approximated as $H = J^T J$, and the gradient is $g = J^T e$. J is a Jacobi matrix containing the first derivative of the error performance function to the networks weights. The function for correct the weights of the networks in LM algorithm is:

$$\omega(n + 1) = \omega(n) - [J^T J + \mu I]^{-1} J^T e \qquad (8)$$

Because the Jacobi matrix is easier to calculate than the Hessian matrix, the LM algorithm can improve the learning efficiency of neural networks.

4 Construction of atmospheric model based on neural networks

The steps of constructing the atmospheric model based on neural networks are as follows:

1. Clean and fusion the measured atmospheric data of GOCE, solar radiation proxy data, and geomagnetic index data. Form integrated data set that includes measured time, longitude, latitude, height, solar radiation proxy, geomagnetic activity index, measured atmospheric density. There are 7954820 samples were collected after eliminating some errors and meaningless data (such as some measured atmospheric density is a minus and some geomagnetic index has no measured value). Since the value space of all kinds of data vary greatly, the data set is normalized linearly based on their maximum and minimum values (Jin et al. 2016);

2. Conduct random classification of the above data set, among which 3000000 samples are randomly selected to form the training data set, and the remaining 4954820 samples are the test data set;

3. Construct neural networks $f(t, longi, lati, Z, SRP, GI) = \rho_{Atmos}$. The neural networks for atmospheric density simulation is set to contain $1 - N$ hidden layers, and the number of node neurons in a single hidden layer is between 5-25 because too many hidden layers and too many neurons in a single hidden layer will increase the computational and application complexity of the neural networks. The training iteration limitation is set as 1000 times. The initial value of the weight matrix IW and $LW(n)(n = 1, 2, \ldots, N)$ in the input layer and hidden layers of neural networks adopts random sequence;

4. Train the neural networks by the training data set in 2). The input parameters of the training sample include time, longitude, latitude, height, $F_{10.7}$ (F_{30}), 81-days mean of $F_{10.7}$ (F_{30}), K_P, and day mean of K_P. The expected output is the atmospheric density at the corresponding time and position. Carried out linear normalization on the input parameters. Add constant term to the input parameters, multiply the input sequence by the weight matrix IW, and carry out the Tan-Sigmoid transform on the input sequence and complete the calculation of the input layer. Make the calculation times of the hidden layer $n = 1$;

5. Add constant term to the input sequence, multiply the transformed input sequence by $LW(n)$ and carry out the Tan-Sigmoid transform to the input sequence, complete the calculation of the $n - th$ hidden layer;

6. If $n = N$, turn to step 7) to the calculation process of the output layer; If $n < N$, make $n = n + 1$, repeat step 5), complete the calculation process of the $n - th$ hidden layer;

7. Since the output layer transform function is linear, no operation is required in the output layer. Carried out reverse linear normalization on the calculation results to obtain the simulation atmospheric density in neural networks;

8. Input the input sequence of the test data set into the trained neural networks. Compare the simulation results with the GOCE measured atmospheric density of the same input sequence, and calculate the mean absolute error rate. If the mean absolute error rate meets the requirements or the number of iterations has reached the limitation, the calculation will stop and turn to step 9); Otherwise, according to the change of gradient, improve various weights in

the weight matrix *IW* and *LW*(*n*) = (*n* = 1, 2, ..., *N*) based on equation (8), re-enter the step 4);

9. Record the weight matrix *IW* and *LW*(*n*)(*n* = 1, 2, ..., *N*) of the last iteration and normalization parameters of the neural networks. The atmospheric model based on neural networks is constructed by the above parameters.

The neural networks were set as 1-4 hidden layers and 5-43 neurons. The neural networks were trained by GOCE training data set 1. Relative to the number of hidden layers and neurons, the curve of model MAE rates was as follows:

It can be seen from Figure 1 that the performance of the neural network changes greatly with the number of hidden layers and the number of neurons increases. For a single hidden layer neural network, the MAE rate drops rapidly and converges as the number of neurons increases. In a neural network with 2 or 3 hidden layers, the MAE rate decreases slowly as the number of neurons increases. In a neural network with 3 hidden layers and 40 neurons, the minimum MAE rate is about 9.6%. As the number of neurons increases continuously, the MAE rate gradually increases. As the number of neurons increases, the MAE rate rises rapidly. This shows that when the hidden layer is more than 3, the entire network is over-fitting. On the contrary, the neural network is under-fitting when the hidden layer is less than 3. Synthesizing the data in the figure, a neural network composed of 3 hidden layers and 40 neurons is optimal.

The MSE (mean square error) variation curve of 1000 training sessions of the atmospheric model based on neural networks is shown in Figure 2.

The atmospheric model training process based on neural networks with 3 hidden layer is shown in Figure 2. When the number of iterations is less than 100 times, the MSE drops rapidly, which shows that the gradient of the network drops quickly and the learning efficiency is high during this period. When the number of iterations exceeds 700, the MSE of the system gradually converges and shrinks to a plateau. This shows that the gradient of the network changes very little and the learning efficiency is very low during this period. The above data shows that it is reasonable to set the upper limit of learning times of the neural network to 1000, and the optimal performance has been reached in the learning of the neural network, and more learning cannot continue to achieve a significant improvement in the performance of the neural network.

5 Simulation Results

The MAE rate of F_{30} proxy neural networks atmospheric model is 9.31%. Figure 3 is the MAE rate after interval sampling.

The MAE rate of $F_{10.7}$ proxy neural networks model is 9.60%. Figure 4 is the MAE rate after interval sampling.

It can be seen from Figure 3 and Figure 4 that the MAE rates of the two neural networks models are extremely approximate. The MAE rate of the atmospheric model based on $F_{10.7}$ neural networks is slightly greater for some outlier data with large errors than that based on F_{30} neural networks. The reason for this phenomenon is that the $F_{10.7}$ proxy will bring greater model error than the F_{30} proxy when the data variance is larger (Cui et al. 2020).

The atmospheric density sampling of GOCE in March 2012 was selected as an example to analyze the accuracy of the two models in a large space range over a long period. The atmospheric density simulation results of the two neural network models corresponding to the GOCE orbital position were compared with the GOCE measured data. The global atmospheric density data measured by GOCE in March 2012 is shown in Figure 5.

The global atmospheric density $F_{10.7}$ neural networks model simulation results in March 2012 is shown in Figure 6.

The global atmospheric density F_{30} neural networks model simulation results in March 2012 is shown in Figure 7.

The MAE rates of the atmospheric model are based on $F_{10.7}$ and F_{30} are 8.18% and 8.07% respectively of the atmospheric density simulation experiment for data in March 2012. It can be seen from Figure 5, Figure 6, and Figure 7 that two neural networks models have completed the reconstruction of atmospheric density data in sampling points. Compared with the measured data, the simulation data of the two neural networks atmospheric models are smoother, and the simulation accuracy of local extremum points is insufficient. In the comparison between the two neural networks models, the simulation results of the local extremum points by the neural networks model based on F_{30} proxy is slightly better than that based on $F_{10.7}$ proxy. As a large number of training data are concentrated on the non-extreme points, the neural network will have the problem of no training or insufficient training for some extreme points. This situation is shown in the figure, which shows that the atmospheric model based on neural network has a poor generalization effect on some extreme points.

To give specific model simulation results, the GOCE measured data for each year from 2009 to 2012 are randomly selected. With the time, longitude, latitude, and altitude in
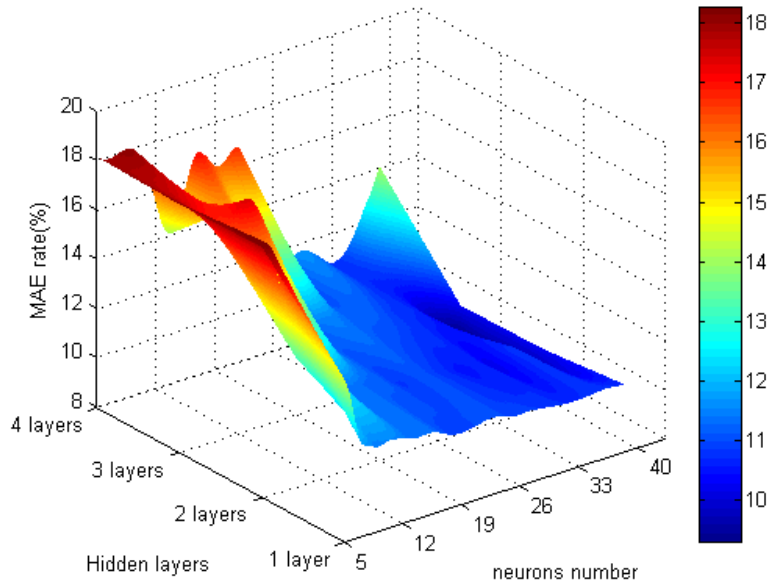
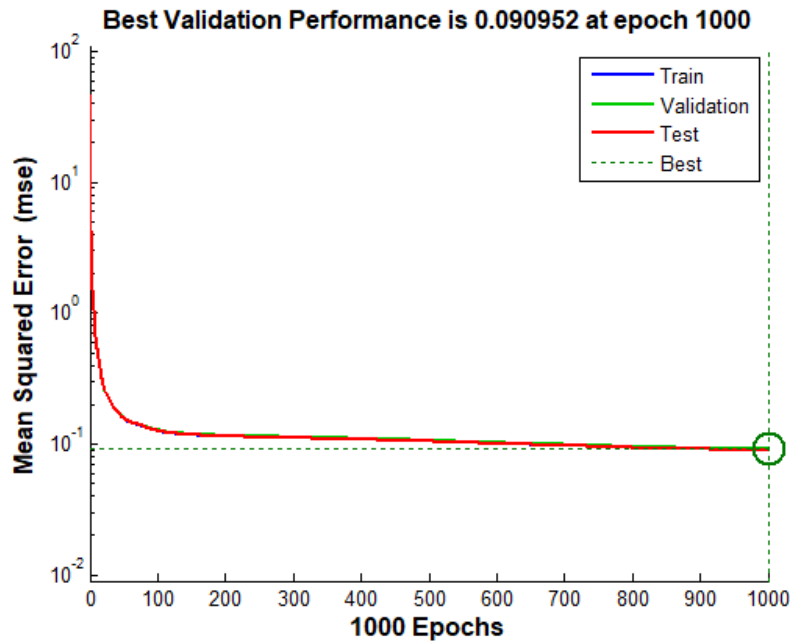**Fig. 1.** The MAE of the neural networks with different hidden layers and neurons

Fig. 2. Neural networks training iteration error graph based on GOCE training data sets

the data as input parameters, the accuracy of the two neural network models and the two traditional atmospheric models were compared. The input parameters are calculated using DTM2013 mode, MSIS00 mode and two neural network atmospheric mode respectively. The randomly selected GOCE measured data input parameters are shown in Table 1.

The GOCE measured atmospheric density and the atmospheric density simulation results of the four models are as shown in Table 2.

The atmospheric density simulation MAE rates of the four models are shown in Table 3.

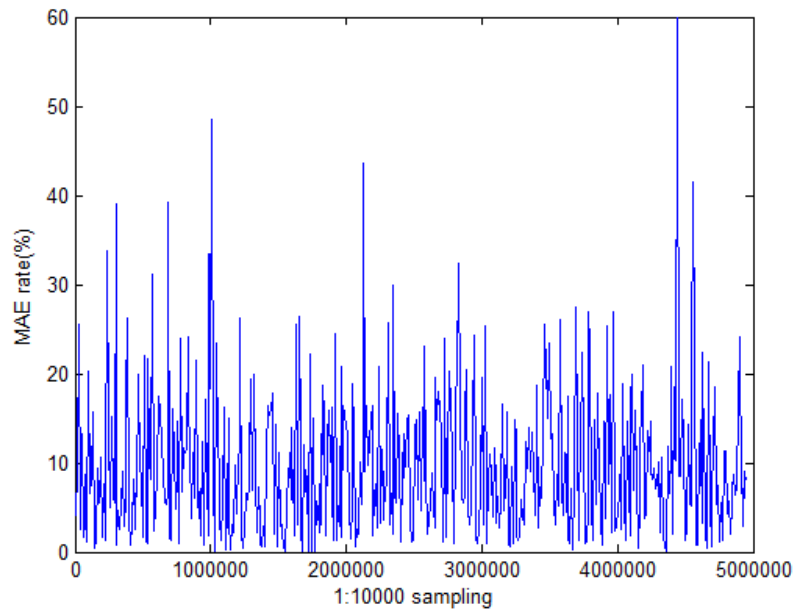The statistical figure of MAE rates of the above four models is shown in Figure 8.

Fig. 3. MAE rate distribution of F_{30} neural networks atmospheric model
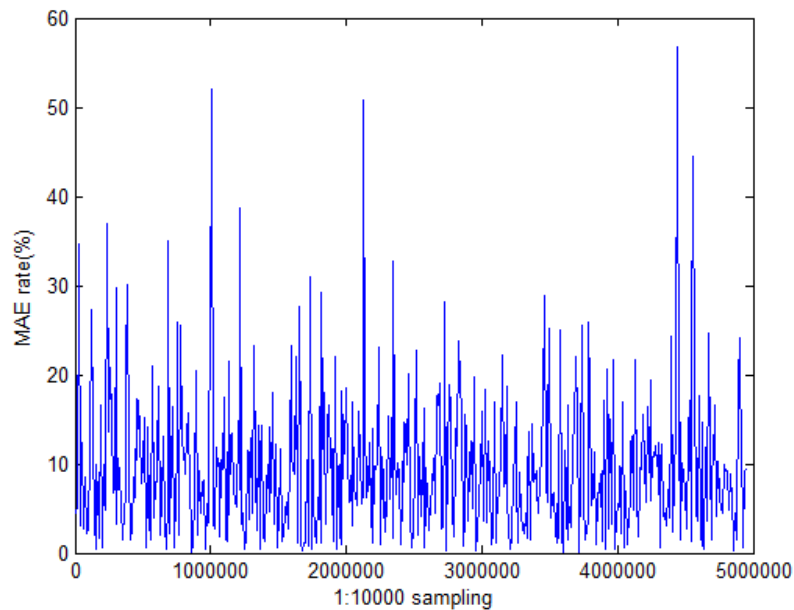

Fig. 4. MAE rate distribution of $F_{10.7}$ neural networks atmospheric model

It can be seen from Table 1, Table 2, Table 3, and Figure 8 that in the simulation results of the atmospheric density of random sampling space locations in different years, the performance of the two neural networks models is significantly better than that of the two traditional atmospheric models. The MAE rates of the neural networks models are about 1/3-1/2 of that of the traditional models. In the two tra-

ditional atmospheric models, the MAE rate of the DTM2013 model is slightly lower than that of the MSIS00 model. In the two atmospheric models based on neural networks, the MAE rate of the F_{30} neural networks model is slightly lower than that of the $F_{10.7}$ neural networks model. For the calculation of atmospheric density at the same time and space, the MAE rates of the two traditional atmospheric
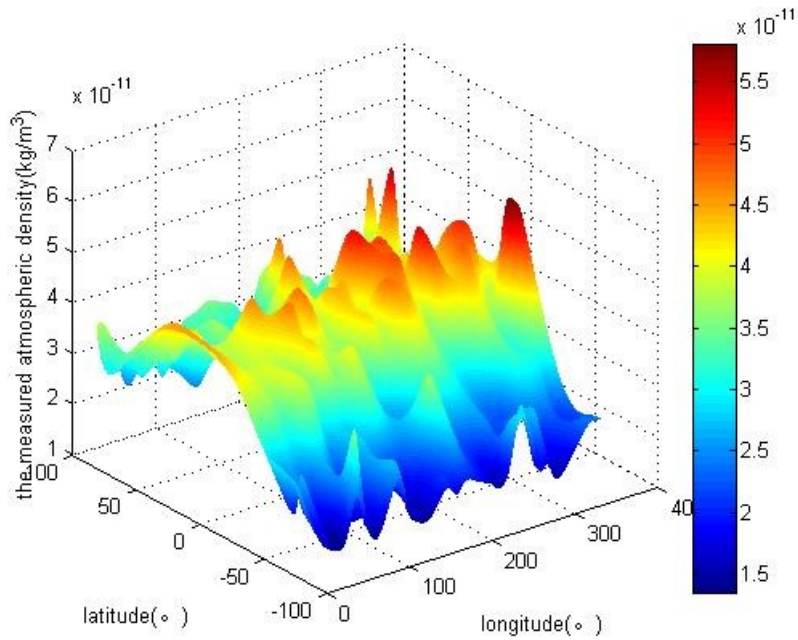
Fig. 5. Global atmospheric density $F_{10.7}$ data measured by GOCE in March 2012
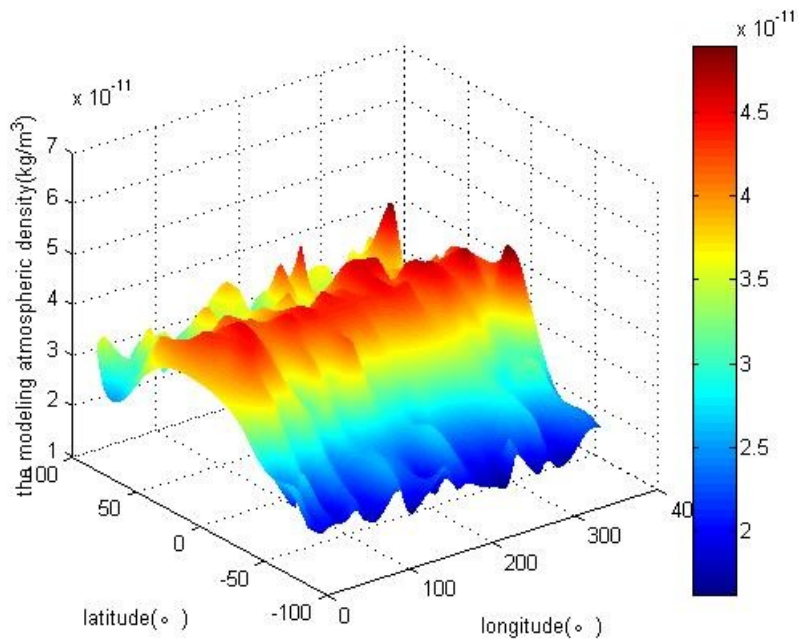

Fig. 6. Global atmospheric density F_{30} neural networks model simulation results in March 2012

models show a certain consistency, and the two neural networks atmospheric models also show a certain consistency. According to equations (1)-(4), the consistency of the two traditional models stems from the fact that the two models are basically the same pattern in calculating atmospheric density. The consistency of the two neural network models stems from the fact that the input parameters and calculation methods of the atmospheric models in the two models are also the same, the difference is only that different solar radiation parameters are used.

It can be seen from equations (1)-(4) that the calculation process of the traditional atmospheric model is as
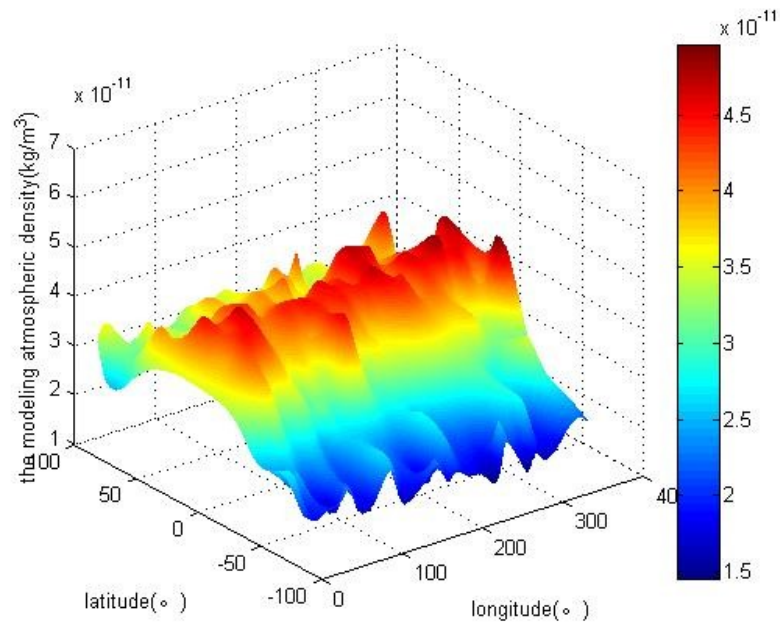
Fig. 7. Global atmospheric density F_{30} neural networks model simulation results in March 2012

Table 1. Input data of GOCE orbit sampled randomly

index	Date&Time	Longitude (°)	Latitude (°)	Height (km)	$F_{10.7}$	$\bar{F}_{10.7}$	F_{30}	$\bar{F}_{30}$	K_P	$\bar{K}_P$
1	2009-11-07 15:06:10.000	57.078	-57.058	287.139	70.90	70.70	47.00	46.60	1	1
2	2009-12-12 08:06:10.000	160.527	-50.927	272.660	72.20	72.90	49.00	49.00	6	5
3	2010-04-12 13:11:30.000	66.282	60.087	269.670	74.500	82.400	52.000	55.500	11	30
4	2010-06-27 04:50:00.000	75.006	81.480	273.966	74.400	73.800	55.000	51.000	51	26
5	2010-11-01 17:00:50.000	27.533	-31.070	271.095	81.20	80.50	57.00	57.10	3	7
6	2011-03-22 13:52:10.000	234.481	-69.731	282.374	100.900	96.200	61.000	62.800	13	11
7	2011-07-27 14:36:30.000	251.167	49.755	263.218	93.40	93.60	61.00	69.10	0	3
8	2011-07-30 17:32:20.000	200.798	11.859	260.824	111.700	93.700	69.00	68.80	30	24
9	2011-12-02 13:00:50.000	267.948	-7.581	262.127	152.40	145.10	100.00	98.50	6	10
10	2012-01-04 07:02:30.000	171.669	47.012	264.095	134.80	146.10	96.00	102.10	2	4
11	2012-05-05 10:22:30.000	324.891	65.761	268.947	113.90	112.30	75.00	76.20	8	3
12	2012-09-28 13:23:30.000	103.207	-68.370	279.995	133.200	121.900	108.000	84.100	14	13

Table 2. The GOCE measured result and Simulation results of four models

index	Date&Time	GOCE Measured result(e-11)	Simulation results of four models(e-11)			
			DTM2013	MSIS00	$F_{10.7}$ NN model	F_{30} NN model
1	2009-11-07 15:06:10.000	0.791684	1.14584	1.40300	0.79150	0.70942
2	2009-12-12 08:06:10.000	1.33798	1.79250	2.20300	1.39692	1.26890
3	2010-04-12 13:11:30.000	3.17176	2.93828	3.25100	2.52090	2.55937
4	2010-06-27 04:50:00.000	2.60328	2.68413	2.31500	2.05854	2.14868
5	2010-11-01 17:00:50.000	2.02270	2.57600	2.44600	1.89619	2.05931
6	2011-03-22 13:52:10.000	1.47715	1.43991	2.04100	1.74983	1.49182
7	2011-07-27 14:36:30.000	2.07180	2.63557	2.43400	2.38089	2.17151
8	2011-07-30 17:32:20.000	2.23447	3.12897	2.88700	2.78608	2.90875
9	2011-12-02 13:00:50.000	4.87579	5.02776	5.31800	5.12038	4.88317
10	2012-01-04 07:02:30.000	3.49073	4.46605	4.29500	3.08013	3.37713
11	2012-05-05 10:22:30.000	3.04203	3.84076	3.68400	3.13390	3.36234
12	2012-09-28 13:23:30.000	2.91271	4.16896	3.31200	2.59259	2.91280

Table 3. MAE rates statistics of atmospheric density simulation of the four models

index	Date&Time	DTM2013	MSIS00	$F_{10.7}$ NN model	F_{30} NN model
1	2009-11-07 15:06:10.000	44.735	77.217	0.023	10.391
2	2009-12-12 08:06:10.000	33.971	64.651	4.405	5.163
3	2010-03-11 13:25:10.000	7.361	2.498	20.520	19.308
4	2010-07-03 19:58:30.000	3.106	11.074	20.925	17.463
5	2010-11-01 17:00:50.000	27.355	20.927	6.255	1.810
6	2011-03-22 13:52:10.000	2.521	38.171	18.460	0.993
7	2011-07-27 14:36:30.000	27.212	17.482	14.919	4.813
8	2011-07-30 17:32:20.000	40.032	29.203	24.686	30.176
9	2011-12-02 13:00:50.000	3.117	9.070	5.016	0.151
10	2012-01-04 07:02:30.000	27.940	23.040	11.763	3.254
11	2012-05-05 10:22:30.000	26.256	21.103	3.020	10.529
12	2012-09-28 13:23:30.000	43.130	13.709	10.990	0.003
	MAE rate	23.895	27.346	11.749	8.671

follows: polynomial fitting is carried out for several factors affecting the atmosphere, the fitting results are summed up, and then the atmospheric temperature is calculated according to the results. Finally, the corresponding atmospheric density is obtained from the atmospheric temperature. But for the atmospheric model based on a neural network, its calculation process is as follows: multiple factors affecting the atmosphere are multiplied by the neural network matrix, then the corresponding atmospheric density can be obtained. The atmospheric model based on neural network does not need to calculate a large number of atmospheric factors fitting polynomials, and does not need to pre-set a large number of atmospheric component coefficients in the algorithm, just need to use the neural network matrix, its calculation process is much simpler than the traditional atmospheric model. On the HP ProLiant DL388 Gen10, the atmospheric model based on neural network performs a single computation in about 1.5-3ms, compared with about 5-7

ms for the traditional atmosphere model. The speed of the neural network atmosphere model is obviously faster than that of the traditional atmosphere model. In the orbit calculation of a low-Earth orbit spacecraft with a height close to GOCE, through the atmospheric model based on the neural network, it is possible to obtain the high-precision atmospheric density of the spacecraft position in quasi real-time and calculate the spacecraft by simply relying on matrix multiplication. The resistance of the device improves the orbit determination accuracy of the device.

6 Conclusion

A novel atmosphere model based on neural networks is derived. In the atmospheric model based on neural networks, the atmospheric density measurement data of GOCE is taken as the basic data. The measured time, longitude,
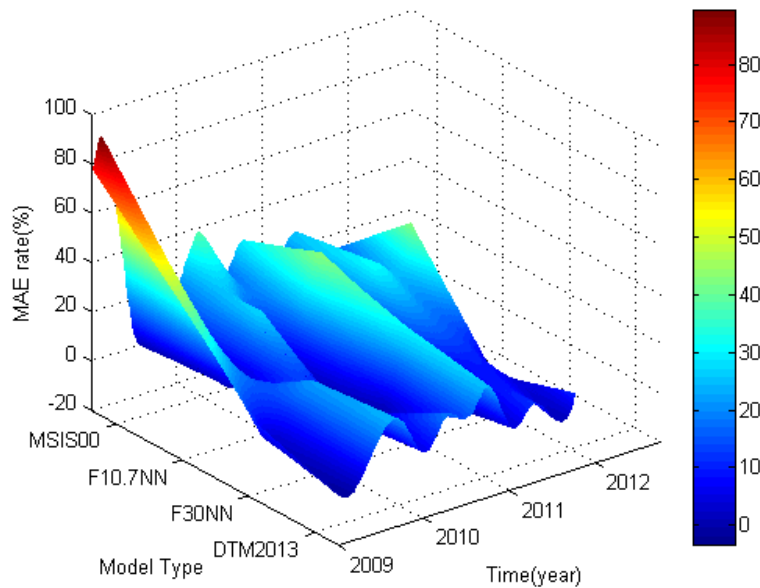
Fig. 8. Simulation MAE rates of 4 models

latitude, height, solar radiation proxies, and geomagnetic indices of the measured space taken as the input parameters, and the atmospheric density of the space position is taken as the label. Compared to the simulation results of the DTM2013 model, the MSIS00 model, and the two neural networks, it is confirmed that the atmospheric model based on neural networks has increased the calculation accuracy significantly and simplified the calculation method significantly. Besides, the atmospheric model based on neural networks can be updated rapidly and iteratively with the new spatial atmospheric measurement data which improves the accuracy of the model. The atmospheric model based on neural network can be applied to orbit determination and orbit prediction of low earth orbit satellites. In the future, if more than one observation is introduced into the method, the range of satellite altitudes that can be applied to it will be expanded. The main limitation of the neural networks model based on GOCE data is that the adaptability of the atmospheric model is limited because the height of GOCE is relatively fixed (about 250-280 km), more measured data of different space height should be added in the future research to wider the adaptability of the model, such as data from satellites such as CHAMP and GRACE. The value of solar radiation proxy $F_{10.7}$ and F_{30} is relatively high compared with the low solar activity years because 2009-2012 is an active period of solar activity. So more measured data of different stages of the solar activity cycle also should be added in the subsequent studies.

Author contribution: Wenhui Cui mainly completed the design of the experiment and the writing of the paper. Min Jiang proofread and revised the paper. Wei Qu and Gang Yao participated in part of the experiment process.

Conflict of interest: There is no conflict of interest in this article.

References

Berger C, Biancale R, Barlier F, Ill M. **1998**. Improvement of the empirical thermosphere model DTM: DTM-94-a comparative review of various temporal variations and prospects in space geodesy applications. J Geod. 72(3):161–178.

Bergstrom S, Proulx R, Cefola P, Nazarenko A, Yurasov V. **2002**. Atmospheric density correction using observational data. Proceedings of the AIAA/AAS Astrodynamics Specialist Conference and Exhibit. Session: ASC-13: Orbital Dynamics and Perturbation Modeling II. Monterey, California. DOI: https://doi.org/10.2514/6.2002-4738

Bruinsma S. **2015**. The DTM-2013 thermosphere model. Journal of Space Weather & Space Climate. 5 A1:A1.

Bruinsma S, Doornbos E, Bowman B. **2014**. Validation of GOCE densities and thermosphere model evaluation. Adv Space Res. 54(4):576–585.

Cao L, Chen X, Misrab AK. **2015**. A novel unscented predictive filter for relative position and attitude estimation of satellite formation. Acta Astronaut. 112:140–157.

Cui W, Qu W, Li H, et al. **2020**. DTM2013 model parameter inversion and correlation analysis between its accuracy. Proceedings of China Satellite Navigation Conference 2020 Volume II: 36-46.

Hatten N, Russell RP. **2017**. A smooth and robust Harris-Priester atmospheric density model. Adv Space Res. 59(2):571–586.

Hedin A, Reber C, Newton G, Spencer NW, Brinton HC, Mayr HG, et al. **1977**. A global thermospheric model based on Mass Spectrometer and Incoherent Scatter Data MSIS 2. Composition. J Geophys Res. 82(16):2148–2156.

Jacchia LG. **1970**. New static models of the thermosphere and exosphere with empirical temperature models. Technical Report 313, Smithsonian Astrophysical Observatory.

Jiang Y. **2018**. Equilibrium points and orbits around asteroid with the full gravitational potential caused by the 3D irregular shape. Astrodynamics. 2(4):361–373.

Jiang Y, Schmidt J, Li H, et al. **2017**. Stable periodic orbits for spacecraft around minor celestial bodies, Astrodynamics. 1-18.

Jin J, Li M, Jin L. **2015**. Data normalization to accelerate training for linear neural net to predict tropical cyclone tracks. Math Probl Eng. 2015(5):1–8.

Liao C, Bai X, Xu M. **2018**. Correction of space atmospheric model based on data mining method. Journal of Beijing University of Aeronautics and Astronautics. 44(12):2628–2636.

Leif S. **1976**. Recalibration of Bartels' geomagnetic activity indices Kp and ap to include universal time variations. J Geophys Res. 81(28):5182–5188.

Lera G, Pinzolas M. **2002**. Neighborhood based Levenberg-Marquardt algorithm for neural network training. IEEE Trans Neural Netw. 13(5):1200–1203.

Li J. **1995**. Satellite precision orbit determination, Beijing: PLA Press. 178-183 (in Chinese).

Marcos F, Bass J, Baker C, Boner W. **1994**. Neutral density models for aerospace applications, In: 32nd Aerospace Sciences Meeting and Exhibit, January 10-13, Reno, NY. DOI: https://doi.org/10.2514/6.1994-589.

McClelland JM, Rumelhart DE, PDP Research Group. Parallel distributed processing, Volume 2. The MIT Press.

Montenbruck O, Gill E. **2001**. Satellite orbits: Models, methods, and applications. Corrected 2nd printing Ed. Springer-Verlag, Berlin.

Picone J, Hedin A, Drob D, Aikin AC. **2002**. NRLMSISIE-00 empirical model of the atmosphere: statistical comparisons and scientific issues. J Geophys Res. 107 A12:SIA 15-1, SIA 15-16.

Rosangela C, Haroldo CV, Juliana A, Steven C. **2015**. Data assimilation by artificial neural networks for the global FSU atmospheric model: Surface Pressure, Conference: 2015 Latin America Congress on Computational Intelligence (LA-CCI).

Tang Y, Hsieh WW, Tang B, Haines K. **2001**. A neural networks atmospheric model for hybrid coupled modelling. Clim Dyn. 17(5-6):445–455.

Wang H, Xiong J, Zhao C. **2014**. The Mid-term forecast method of solar radiation index F10.7. Journal of Astronautics. 55(4):302–312. [in Chinese].

Xu J, Zhang GX. **2018**. Design and transmission performance analysis of satellite constellation for broadband LEO constellation satellite communication system based on high elevation angle. IOP Conf Series Mater Sci Eng. 452:042092.

Zhang T, Li Z, Li J. **2014**. An adaptive genetic algorithm for solving ground-space TT&C resources Integrated scheduling problem of Beidou constellation. Proceedings of 2014 IEEE Chinese Guidance, Navigation and Control Conference. 1785-1792.